

Shock'n on Shakers

George Fox Lang, Associate Editor

Electrodynamic and hydraulic shakers have become a commonly used platform for shock testing. This article reviews current controller technology to safely and reliably compensate for the mechanical limitations of both types of shakers in reproducing desired shock excitations.

Controlled hydraulic and electrodynamic shakers have become the preferred test platforms for modest shock tests. While drop-test (and other) facilities remain necessary for the simulation of extreme shock pulses, the controlled shaker has proven very cost effective for more routine product qualification and seismic evaluation work. Modern DSP shaker controllers now do an outstanding job of reproducing desired transient pulses safely, reliably and repeatably. Their use saves the enormous time of iteratively designing mechanical drop-targets to provide a required shock profile. One now merely keys in or selects the desired acceleration-versus-time shock profile or its shock response spectrum (SRS) and runs the test.

However, a shaker presents some physical barriers to shock testing. These devices have a limited range of displacement stroke and exhibit velocity limits (valve or amplifier induced) that cannot be exceeded without loss of control. The shaker controller compensates for these shortcomings by employing a process termed 'compensation,' the focus of this article. While this compensation process is not without flaws, it opens the range of testing that can be performed on a single laboratory system enormously.

The Problem

Shock test profiles are typically described by an acceleration-versus-time history of a few milliseconds duration. Certain shapes have become the Classical Shock library. These basic pulse forms stem from prior drop-testing wherein the test object starts in free-fall and collides with a target whose elastic and crush properties determine the test acceleration profile. The resulting pulse shapes are almost invariably unipolar as displacement and velocity were not considerations in their development. When these same profiles are run on a shaker, velocity and displacement are the primary concern.

Consider the classic half-sine acceleration shock pulse shown in Figure 2. Since the acceleration is solely in the positive direction, the velocity at the pulse's conclusion is positive and the test object continues to move at this velocity even though the acceleration has returned to zero. The test object has displaced during the shock pulse and will continue to displace at constant velocity until arrested by some barrier. Without smarter intervention, the stroke limits of a shaker could provide this barrier with likely expensive and dangerous results.

A shaker can only operate over a limited range of displacement, its stroke. Within this range it can only operate in a controlled fashion if its velocity limit is not exceeded. Available amplifier-voltage limits the maximum controlled velocity of an electrodynamic shaker, while the flow gain of the control valve dictates the velocity limit of a hydraulic shaker.

Hence, a shock-test can only be run if the resulting displacements fall within the shaker's stroke range with peak velocity within system limits. As a matter of practicality, the test must start from conditions of zero acceleration, velocity and displacement and return to this state at the conclusion. This can be accomplished by the use of pulse compensation, which is automatically introduced by the controller. Most controllers also perform a feasibility analysis before attempting to conduct the test and will stop impractical application without risking the shaker system in any way.

Classical Pulses and their Properties

You will note that the motional responses of Figure 2 were presented in normalized form. Time was divided by the pulse duration T , acceleration was divided by the peak acceleration A , velocity was divided by AT and displacement by AT^2 . These normalizations are industry-standards, allowing an acceleration pulse and its integrals to be easily over-plotted within a reasonable graphic range, without concern for the peak value of the pulse or its duration or the system of measurement units employed.

The terminal normalized acceleration, velocity and displacement values of such a plot are termed k_A , k_V and k_D , respectively. These coefficients permit a simple and industry-accepted means of describing the gross motional characteristics of a shock-pulse. Graphical Table 1 presents these coefficients (and others) for a variety of *Classical Shock* waveforms, including those employed in compensation.

The motional changes induced by a pulse of Table 1 may be converted to a physical unit basis in accordance with:

$$\text{Acceleration change} = k_A A \quad (1)$$

$$\text{Velocity change} = k_V AT \quad (2)$$

$$\text{Displacement change} = k_D AT^2 \quad (3)$$

Note that all pulses in this table start and end at zero acceleration. For this reason, each has a k_A coefficient of zero. Pulses with non-zero k_A will be discussed subsequently. Table 1 also includes two less common indicators, k_{SE} and k_{ME} . These will be discussed in context of a spectral representation of the pulses. These indices may be converted to physical units in accordance with:

$$\text{Signal Energy} = k_{SE} A^2 T \quad (4)$$

$$\text{Mechanical Energy} = k_{ME} M A^2 T^2 \quad (5)$$

where M is the mass of the test object

Our focus now returns to utility of the three motional coefficients k_A , k_V and k_D . At time = t_0 , the displacement, velocity and acceleration of the object under test are y_0 , \dot{y}_0 and \ddot{y}_0 , respectively. Applying a pulse of amplitude A and duration T changes all of these parameters. At the conclusion of the pulse, these state-variables relate to the initial conditions in accordance with:

$$\begin{Bmatrix} 1 \\ t \\ y \\ \dot{y} \\ \ddot{y} \end{Bmatrix} = \begin{bmatrix} 1 & 0 & 0 & 0 & 0 \\ T & 1 & 0 & 0 & 0 \\ k_D AT^2 & 0 & 1 & T & T^2/2 \\ k_V AT & 0 & 0 & 1 & T \\ k_A A & 0 & 0 & 0 & 1 \end{bmatrix} \begin{Bmatrix} 1 \\ t_0 \\ y_0 \\ \dot{y}_0 \\ \ddot{y}_0 \end{Bmatrix} \quad (6)$$

In our initial considerations, we will deal with pulses characterized by $k_A = 0$ and we can simplify the state relationships to:

$$\begin{Bmatrix} 1 \\ t \\ y \\ \dot{y} \end{Bmatrix} = \begin{bmatrix} 1 & 0 & 0 & 0 \\ T & 1 & 0 & 0 \\ k_D AT^2 & 0 & 1 & T \\ k_V AT & 0 & 0 & 1 \end{bmatrix} \begin{Bmatrix} 1 \\ t_0 \\ y_0 \\ \dot{y}_0 \end{Bmatrix} \quad (7)$$

Eq. 7 will provide the basis to understand shock-pulse compensation.

Bouncing Back – Basic Compensation

Figure 2 illustrates application of a half-sine pulse to a test



Figure 1. Shock testing on an electrodynamic shaker. Mars Exploration Rover #1 undergoing vertical axis landing loads pulse testing at JPL on an LDS Model 994 shaker. Photo courtesy of the Jet Propulsion Laboratory, California Institute of Technology.

object initially at equilibrium. At the conclusion of the pulse, the specimen is displaced positively and moving with a positive velocity. This can be modeled by Eq. 7 and the coefficients of Table 1 as:

$$\begin{Bmatrix} 1 \\ t \\ y \\ \dot{y} \end{Bmatrix}_{T_A} = \begin{Bmatrix} 1 \\ T_A \\ 0.3183AT_A^2 \\ 0.6366AT_A \end{Bmatrix} = \begin{Bmatrix} 1 & 0 & 0 & 0 \\ T_A & 1 & 0 & 0 \\ 0.3183AT_A^2 & 0 & 1 & T_A \\ 0.6366AT_A & 0 & 0 & 1 \end{Bmatrix} \begin{Bmatrix} 1 \\ 0 \\ 0 \\ 0 \end{Bmatrix} \quad (8)$$

Clearly, we need to do something to arrest the motion if this test is to be conducted on a shaker. The obvious solution is to apply a pulse of opposite sign. To comply with the test specifications, this added pulse should be low in amplitude. For sake of example, let's restrict this pulse to be no more than 20 percent of the amplitude of the test pulse. For a given peak amplitude, the most influential pulse we can use is a rectangle. This can be concluded by examining the k_V and k_D factors in

Table 1. Classical shock pulses and various non-dimensional properties.

<p>rectangle</p> <p>$k_A = 0.0$ $k_V = 1.0$ $k_D = 0.5$ $k_{SE} = 1.0$ $k_{ME} = 0.5$</p>	<p>Fandrich</p> <p>$k_A = 0.0$ $k_V = 0.7797$ $k_D = 0.3898$ $k_{SE} = 0.6855$ $k_{ME} = 0.5$</p>
<p>terminal-pk sawtooth</p> <p>$k_A = 0.0$ $k_V = 0.5$ $k_D = 0.1667$ $k_{SE} = 0.3333$ $k_{ME} = 0.125$</p>	<p>initial-peak sawtooth</p> <p>$k_A = 0.0$ $k_V = 0.5$ $k_D = 0.3333$ $k_{SE} = 0.3333$ $k_{ME} = 0.125$</p>
<p>triangle</p> <p>$k_A = 0.0$ $k_V = 0.5$ $k_D = 0.250$ $k_{SE} = 0.3333$ $k_{ME} = 0.125$</p>	<p>trapezoid</p> <p>$k_A = 0.0$ $0.5 < k_V < 1.0$ $1.667 < k_D < 0.5$ $0.333 < k_{SE} < 1.0$ $0.125 < k_{ME} < 0.5$</p>
<p>half-sine</p> <p>$k_A = 0.0$ $k_V = 0.6366$ $k_D = 0.3183$ $k_{SE} = 0.5$ $k_{ME} = 0.2026$</p>	<p>haversine</p> <p>$k_A = 0.0$ $k_V = 0.5$ $k_D = 0.250$ $k_{SE} = 0.375$ $k_{ME} = 0.125$</p>
<p>sine</p> <p>$k_A = 0.0$ $k_V = 0.0$ $k_D = 0.1591$ $k_{SE} = 0.5$ $k_{ME} = 0.0$</p>	<p>damped sine</p> <p>$k_A = 0.0$ $0.0 < k_V < k_D$ $0.0 < k_D < 0.1591$ $0.0 < k_{SE} < 0.5$ $0.0 < k_{ME} < 0.007976$</p>

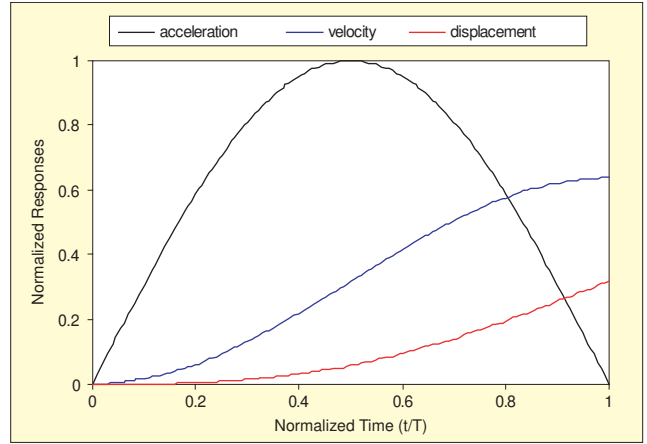


Figure 2. Normalized responses to a half-sine acceleration pulse. Black – acceleration/A, blue – velocity/AT, red – displacement/AT².

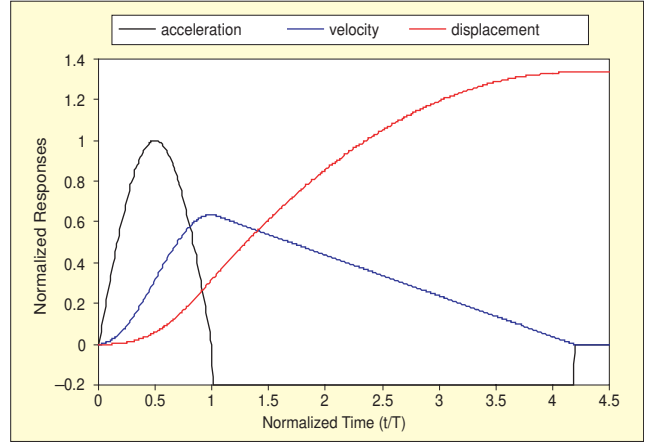


Figure 3. Using a negative pulse to drive the velocity to zero leaves a positive displacement of the shaker armature.

Table 1; those for a *rectangle* are the largest.

We again apply Eq. 7, now using the *rectangle* k_V and k_D factors in the matrix and the results of Eq. 8 as the input state-vector. The results are:

$$\begin{Bmatrix} 1 \\ T_B \\ -0.5BT_B^2 \\ -BT_B \end{Bmatrix} \begin{Bmatrix} 1 \\ 0 \\ 0 \\ 0 \end{Bmatrix} \begin{Bmatrix} 1 \\ T_A \\ 0.3183AT_A^2 \\ 0.6366AT_A \end{Bmatrix} = \begin{Bmatrix} 1 \\ T_A + T_B \\ 0.3183AT_A^2 + 0.6366AT_A T_B - 0.5BT_B^2 \\ 0.6366AT_A - BT_B \end{Bmatrix} \quad (9)$$

Clearly, to arrest motion, the terminal velocity must equate to zero. That is, the added negative rectangle must be of such duration that the area above its curve equals that of the area under the initial half-sine test pulse. That is:

$$\dot{y}_{T_A+T_B} = 0.6366AT_A - BT_B = 0 \Rightarrow T_B = 0.6366 \frac{A}{B} T_A \quad (10)$$

However, we also want the shaker to come to rest at its original mid-stroke position. If we fail in this quest, the controller is obligated to hold the shaker at an offset position by applying a DC command . . . forever! The displacement at the end of the pulse, where velocity is zero, is given by:

$$y_{T_A+T_B} = 0.3183AT_A^2 + 0.6366AT_A T_B - 0.5BT_B^2 = 0.3183AT_A^2 \left(1 + 0.6366 \frac{A}{B} \right) \quad (11)$$

This is clearly a non-zero result. For a 20% compensation

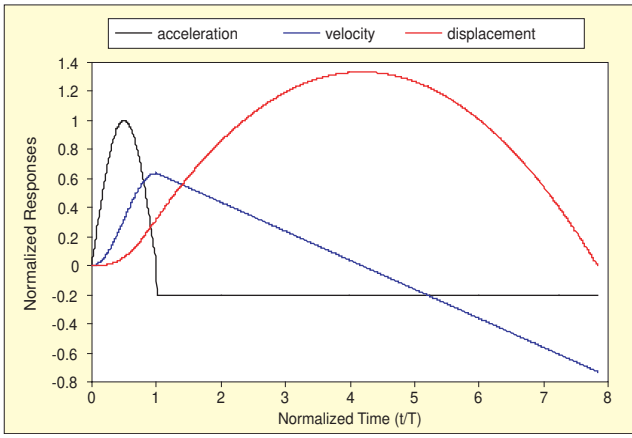


Figure 4. Using a longer negative pulse to drive the displacement back to zero leaves a negative velocity at that point.

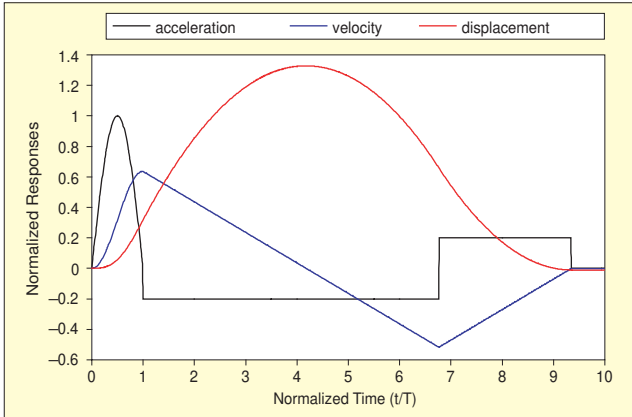


Figure 5. Applying a negative 20% amplitude rectangle pulse 5.763 times as long as the half-sine, followed by a positive 20% pulse 2.580 times as long, returns the shaker to mid-stroke at zero velocity and acceleration in 9.343 half-sine durations.

pulse ($B = 0.2A$) the rest position of the shaker is:

$$y_{T_A+T_B} = 1.3314AT_A^2.$$

This result is illustrated in Figure 3.

Simply increasing the duration of the compensating pulse will not correct the problem. The shaker could be driven to zero displacement, but would arrive there with considerable negative velocity as illustrated by Figure 4.

The solution to this conundrum is not intuitively obvious. The answer is to apply the negative pulse for *longer* than necessary to bring the velocity to zero, then apply a positive pulse to drive the velocity back to zero. This solution is illustrated in Figure 5. Note the terminal state has zero acceleration, velocity and displacement.

The duration of the compensating pulses cannot be chosen capriciously. Again apply Eq. 7, this time with a matrix representing a *positive* rectangular pulse acting upon the input state-vector provided by Eq. 9 to achieve the final post-test state. Specifically:

$$\begin{Bmatrix} 1 & 0 & 0 & 0 \\ T_C & 1 & 0 & 0 \\ 0.5CT_C^2 & 0 & 1 & T_C \\ CT_C & 0 & 0 & 1 \end{Bmatrix} \begin{Bmatrix} 1 \\ T_A + T_B \\ 0.3183AT_A^2 + 0.6366AT_AT_B - 0.5BT_B^2 \\ 0.6366AT_A - BT_B \end{Bmatrix} = \begin{Bmatrix} 1 \\ T_A + T_B + T_C \\ \left[\begin{array}{l} 0.5CT_C^2 + 0.3183AT_A^2 + 0.6366AT_AT_B \\ -0.5BT_B^2 + 0.6366AT_AT_C - BT_B T_C \\ CT_C + 0.6366AT_A - BT_B \end{array} \right] \end{Bmatrix} \quad (12)$$

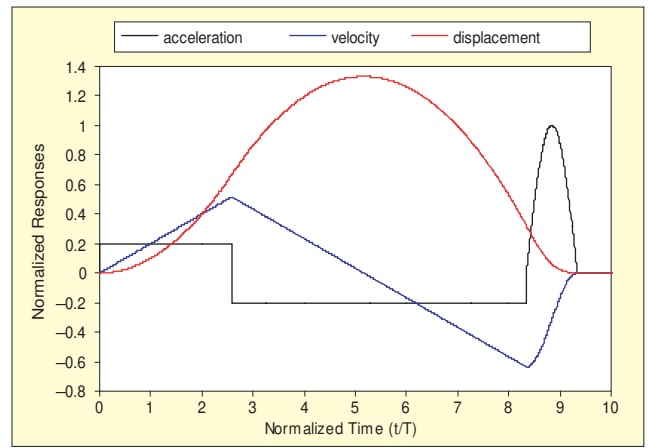


Figure 6. Preceding the half-sine by a positive rectangular pulse of 20% amplitude and 2.580 times duration, followed by a negative 20% amplitude pulse 5.763 as long, leaves the shaker at mid-stroke with zero velocity and acceleration in 9.343 durations.

We require the terminal velocity and displacement to be zero. That is:

$$\dot{y} = CT_C + 0.6366AT_A - BT_B = 0 \quad (13)$$

$$\begin{aligned} y &= 0.5CT_C^2 + 0.3183AT_A^2 + 0.6366AT_AT_B \\ -0.5BT_B^2 + 0.6366AT_AT_C - BT_B T_C &= 0 \end{aligned} \quad (14)$$

For simplicity, we have used compensation pulses of equal amplitude and opposite signs. That is, $B = C = 0.2A$. Imposing this simplification on Eqs. 13 and 14 results in the simultaneous solutions:

$$T_B = 5.736T_A \quad (15)$$

$$T_C = 2.580T_A \quad (16)$$

As intuition would suggest, these same solution times can be used for a pre-pulse compensation as illustrated in Figure 6. When we reverse the sequence of pulses in time, the state-vectors are different. The terminal state-vector for the test of Figure 6 is given by Eq. 17.

$$\begin{Bmatrix} 1 \\ t \\ y \\ \dot{y} \end{Bmatrix} = \begin{bmatrix} 1 & 0 & 0 & 0 \\ T_A & 1 & 0 & 0 \\ 0.3183AT_A^2 & 0 & 1 & T_A \\ 0.6366AT_A & 0 & 0 & 1 \end{bmatrix} \begin{Bmatrix} 1 & 0 & 0 & 0 \\ T_B & 1 & 0 & 0 \\ -0.5BT_B^2 & 0 & 1 & T_B \\ -BT_B & 0 & 0 & 1 \end{Bmatrix} = \begin{Bmatrix} 1 \\ T_C & 1 & 0 & 0 \\ 0.5CT_C^2 & 0 & 1 & T_C \\ CT_C & 0 & 0 & 1 \end{Bmatrix} \begin{Bmatrix} 1 \\ 0 \\ 0 \\ 0 \end{Bmatrix} \quad (17)$$

$$\begin{Bmatrix} 1 \\ T_A + T_B + T_C \\ \left[\begin{array}{l} 0.3183AT_A^2 - 0.5T_B^2 + 0.5CT_C^2 + CT_B T_C - BT_A T_B + CT_A T_C \\ 0.6366AT_A - BT_B + CT_C \end{array} \right] \end{Bmatrix}$$

Again we demand the terminal velocity and displacement to be zero. That is:

$$\dot{y} = CT_C + 0.6366AT_A - BT_B = 0 \quad (18)$$

and

$$\begin{aligned} y &= 0.5CT_C^2 + 0.3183AT_A^2 - BT_A T_B \\ -0.5BT_B^2 + CT_A T_C + CT_B T_C &= 0 \end{aligned} \quad (19)$$

While the velocity of Eq. 18 is identical to that of the post-pulse compensation constraint of Eq. 13, the displacement of Eq. 19 differs from the corresponding constraint, 14. Nonetheless, the solutions previously stated in 15 and 16 satisfy Eqs. 18 and 19.

This simple exercise has highlighted several important observable facts:

1. Compensation is *not* an option; it is *absolutely required* to run an unipolar shock pulse on an electrodynamic or hydraulic shaker.
2. Compensation pulses may be added either before or after the test-pulse to force the test to both start and end at zero acceleration, velocity and displacement.
3. In general, *two* pulses of opposite sign must be added to bring both terminal velocity and displacement back to zero.
4. The compensation pulses may be of much lower amplitude than the desired test pulse (and they need not be of equal amplitude to one another). They do not need to have the same shape as the test pulse.
5. The lower the amplitude of the compensation pulses, the longer the total controlled-pulse duration will become. (This can pose a controller problem.)
6. Maximum stroke and velocity occur *outside* the desired test pulse, within the compensation interval.
7. When (exclusive) pre- or post-pulse compensation is used, only half of the available shaker stroke will be utilized.

First, Last or Both?

Should I compensate before or after my specified test pulse? Is there any merit in doing both? These are two very perceptive questions, each suffering test-specific answers.

Shock tests are run for a variety of reasons. Some profit from pre-test compensation, some from post-test compensation. If the shock is large with respect to the shaker's capability, these specific advantages may need to be set aside. A combination of pre- and post-pulse compensation may be required, simply to allow the shaker to generate the pulse within its stroke and velocity limits.

Consider qualification of an air-bag deployment sensor. The shock-test is likely run to determine the g-level at which the sensor switch closed, causing bag detonation. In this situation, a clear picture of events during the test-pulse rise is required. Post-pulse compensation is the right answer here, providing an uncontaminated rising input from the desired zero-g initial condition.

Now consider testing a computer disk drive, obliged to operate in a hostile travel environment. The shock-test is likely to include monitoring read/write functioning through and after the simulated bump. In this instance, pre-pulse compensation is the right answer so that 'aftershock' effects raise no question of continued proper function.

Other tests are more pedantic – they are merely run to demonstrate the test object can survive the event and this determination is not made during the shock-test. Here the use of pre or post-pulse compensation is a moot point. However, test labs are always called upon to simulate increasingly hostile environments without commensurate upgrade of the available test facilities. Eventually, you will be faced with running a pulse too aggressive for the half-stroke of your shaker, or one that requires peak velocity beyond its control range. This is where combined pre- and post-pulse compensation can save the day.

Figure 7 illustrates combined pre- and post-pulse compensation of a half-sine using equal amplitude trapezoidal compensation pulses of 20% amplitude. Compare this with Figures 5 and 6 that illustrate the same test-pulse and note:

1. The peak displacement values are centered about the shaker's mid stroke, doubling the available displacement range.
2. The total peak-to-peak stroke used is significantly less than that of a pre- or post-pulse (only) compensated test.
3. The peak velocities are significantly lower for the pre- and post-compensated test.
4. The total controlled-pulse times are all about equal.

At first blush, this all seems too good to be true. However, it is the natural result of using shorter compensation pulses. In fact, the symmetric solution presented is far from optimum. Modern controllers can combine a myriad of pulse shapes to provide optimization for stroke, velocity *and the energy im-*

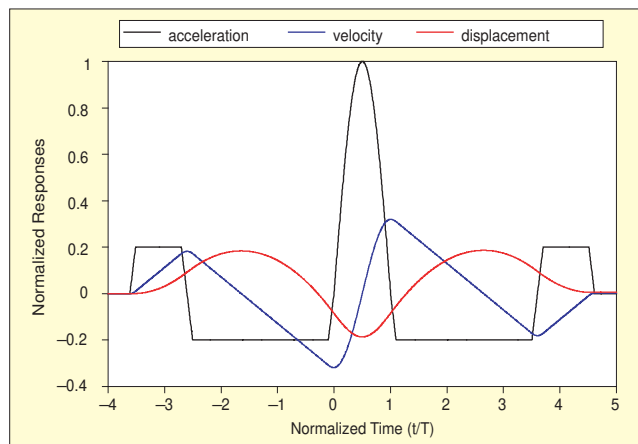


Figure 7. An example of combined pre- and post-pulse compensation using four equal-amplitude trapezoidal pulses. Note symmetric stroke and velocity peaks.

posed on the test object.

By using two preceding and two following pulses (or following pulses of asymmetric nature), the controller can position the shaker armature to a negative displacement prior to the test-pulse with a negative velocity equal to about half of the velocity change induced by the desired test waveform. It will select these pulses so that the stroke used is centered in the shaker's range. Thus, a modern controller allows the shaker system to deliver the most aggressive test-pulse possible within its physically limited stroke and velocity capabilities.

Why All of These Pulse Shapes?

The half-sine, haversine, triangle, trapezoid, terminal-peak sawtooth and initial-peak sawtooth are all elements of the *Classical Shock* waveform library. (I should note here that the rectangle, triangle and sawtooth waveforms are all specific sub-sets of the trapezoid, determined by the *rise-time* and *fall-time* durations.) Each of these pulse-shapes has a place in the history of shock-testing and each is the likely focus of your next specified test, being someone's notion of the proper simulation of an environmental event your product is likely to suffer.

In contrast, the rectangle, Fandrich, sine and damped-sine pulses are all typically employed as *compensation pulses*. Each has desirable characteristics in the eyes of the *test feasibility* designer. R. T. Fandrich¹ may have been the prototype *test feasibility* designer. In 1981 he studied the problem of performing a MIL-STD-810C half-sine pulse of 30 g peak and 11 msec duration on an electrodynamic shaker with a 1 in. PTP stroke. His solution is embedded in many controllers and spawned a host of independently invented, improved solutions to the general problem.

One of Fandrich's concerns was the *additional* damage potentially induced by the compensating pulses. While he admired the positioning efficiency of the rectangular pulse, he feared its rich spectral content (caused by the abrupt rising and falling edges) might induce unwarranted stress in the test object. His solution was to approximate the square pulse with only first and third harmonic components. (Note that his solution is not simply the truncation of Fourier Coefficients for a rectangular pulse.) He chose to approximate a rectangular pulse of amplitude A and duration T by:

$$\ddot{y}(t) = 1.155 \sin\left(\pi \frac{t}{P}\right) + 0.231 \sin\left(3\pi \frac{t}{T}\right) \quad (20a)$$

for $0 < t < T$ and 0 elsewhere

I believe that Mr. Fandrich relied heavily on numerical integration in his landmark work. I respectfully submit that a closed-form solution provides a slightly more precise statement, which is:

$$\ddot{y}(t) = 1.148342 \left[\sin\left(\pi \frac{t}{P}\right) + \frac{1}{5} \sin\left(3\pi \frac{t}{T}\right) \right] \quad (20b)$$

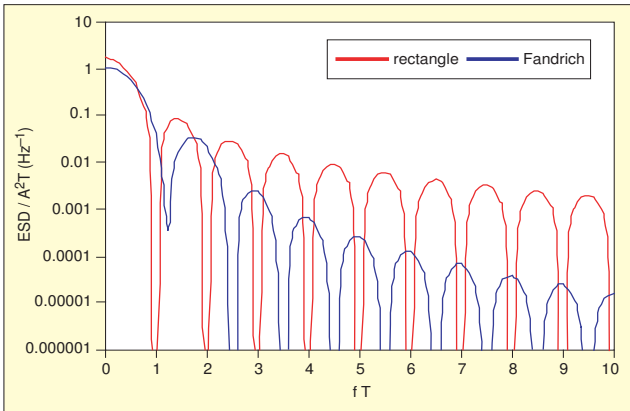


Figure 8. Comparison of the normalized energy spectral density of a rectangle and Fandrich pulse of the same peak amplitude and duration.

Indeed, the Fandrich pulse has less frequency content than a rectangular pulse, although the difference may be less profound than the equation suggests. Figure 8 compares the *Energy Spectral Density* spectra of a Fandrich pulse and rectangular pulse of the same peak amplitude and duration. Clearly, the Fandrich pulse attenuates more rapidly as frequency increases. Also clear is the fact that this pulse (like the rectangle) contains distributed energy across a wide band, not merely content at two frequencies.

The rectangle spectrum exhibits a zero at every frequency multiple of $1/T$. The first lobe is -13.4 dB below the DC value and subsequent lobes roll-off at -6 dB/octave. The Fandrich pulse has a wider primary lobe; with the first zero at $1.25/T$. Subsequent zeros occur at $2.5/T$, $3.5/T$ and so on. The first side-lobe amplitude is -14.8 dB less than the primary lobe and subsequent side-lobes decay at -12 dB/octave.

Mr. Fandrich also proposed the use of a damped-sine as a post-pulse compensation. He chose this single asymmetric pulse as an alternative to two post-test compensation pulses of opposite sign. The intent here was to have a single pulse with k_D/k_V ratio selectable by specifying the damping factor. You will note from Table 1 that the (undamped) sine is unique in exhibiting a k_V of zero. As damping is applied, this rises rapidly relative to k_D . It is interesting to note that Fandrich prescribed an unusual damped-sine equation of the form:

$$\ddot{y}(t) = t^p \sin\left(2\pi \frac{t}{T}\right) \text{ for } 0 < t < T, \text{ 0 elsewhere} \quad (21)$$

He describes evaluating this for positive exponent p and then applying the waveform in time-reversed sequence. Unfortunately, evaluating closed-form solutions for k_V and k_D of this waveform is difficult; an infinite series of sub-integrals results. Table 1 presents a more conventional damped-sine (in vibration parlance) description in accordance with:

$$\ddot{y}(t) = e^{-2\pi\delta t/T} \sin\left(2\pi \frac{t}{T}\right) \text{ for } 0 < t < T, \text{ 0 elsewhere} \quad (22)$$

Figure 9 illustrates typical normalized responses of the conventional damped-sine of Table 1. This plot presents responses with a damping factor of $\delta = 0.375$. k_V and k_D may be tuned by selecting δ in accordance with:

$$k_V = \frac{1 - e^{-2\pi\delta}}{2\pi(1 + \delta^2)} \quad (23)$$

and

$$k_D = \frac{1 - 2\delta k_V}{2\pi(1 + \delta^2)} \quad (24)$$

Figure 10 illustrates k_D , k_V and their ratio as a function of selected damping factor δ .

Some More Recent Contributions

In the 22 years since the landmark Fandrich paper, control-

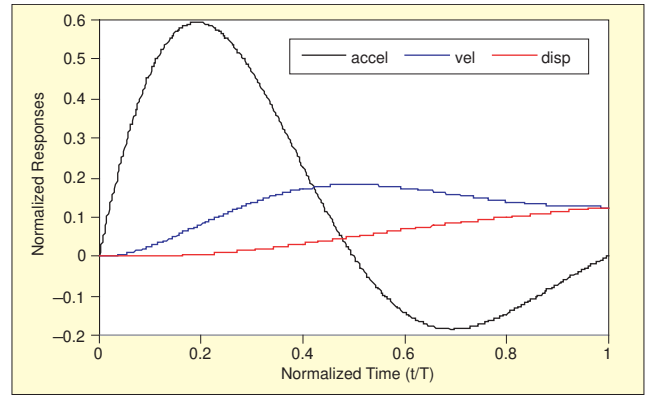


Figure 9. Normalized acceleration, velocity and displacement responses of a damped-sine for damping value, $\delta = 0.315$.

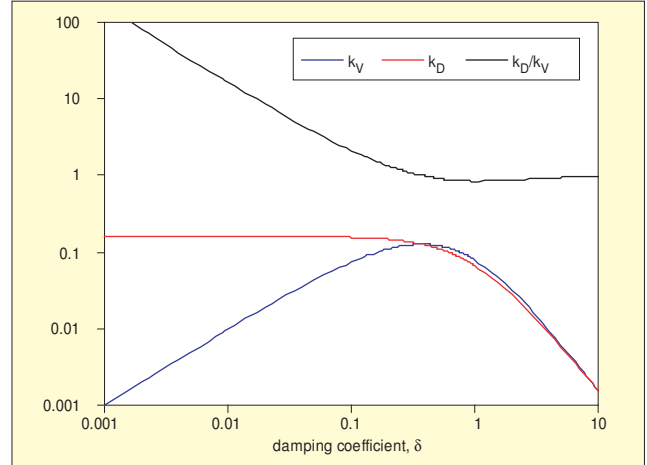


Figure 10. Range of damped-sine k_D and k_V coefficient variation provided by selection of damping factor, δ .

ler designers have been busy. In addition to the daunting task of porting shaker control from dedicated racks to friendly personal computer screens, some designers have returned to the basic physics of the problem.

One area of recent exploitation is the use of pulses with non-zero k_A coefficients. For example, consider the half-sine pulse previously discussed. Allow this pulse to ‘overshoot’ by evaluating it for more than a half-cycle excursion as shown in Figure 11.

This allows the test-pulse itself to be part of the post compensation. As the sine function passes through zero, its slope is nearly constant. Extending the pulse by 10% provides a very linear decrease in acceleration to -0.30 of the pulse magnitude. This is in the ‘neighborhood’ of the post-pulse level that must be applied to meet MIL-STD-810 requirements. One gets to that level with no further curve inflections, minimizing spectral content due to compensation.

Since the pulse no longer starts and ends at the same acceleration, a non-zero k_A equal to the terminal normalized acceleration results. The pulse sequence is obligated to contain another asymmetric pulse with equal and opposite k_A to return the shaker to zero acceleration at the test end. This can be as simple as a ramp between the terminal value and zero, perhaps with a sine (or other waveform) added to it. Alternatively, a partial sine cycle might be selected as the (single) complementary post-test pulse.

As shown in Figure 12, the variation of k_A with overshoot is highly linear up to 30% of the test-pulse amplitude, owing to the near-linear slope of a sine passing through zero. When pulses with non-zero k_A are included in the test sequence, the general state-vector of Eq. 6 applies in lieu of the simplified statements of Eq. 7.

It is refreshing to see that the refinement of shock-test control still includes return to the basic physics of the problem.

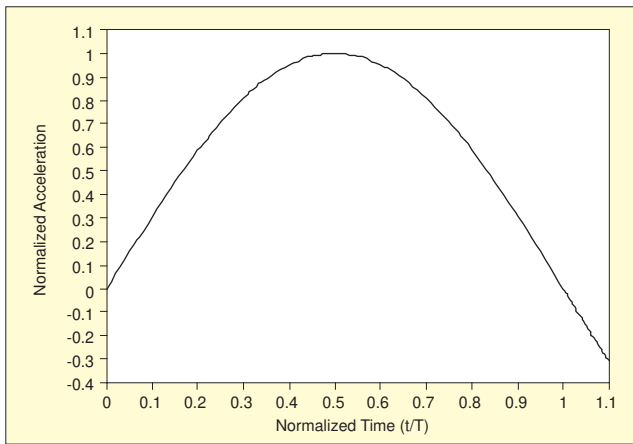


Figure 11. Half-sine pulse with 10% period overshoot ends at $-0.3A$ acceleration level.

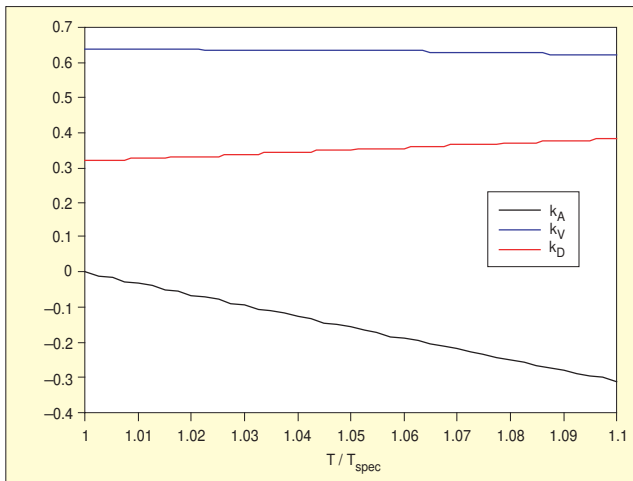


Figure 12. Variation of k_A , k_V and k_D coefficients with overshoot of half-sine period.

We all appreciate the advancements PCs offer, but only when the underlying solution is technically astute!

An Art-State Audit

I have alluded to continued development effort in this field and feel obliged to provide some hard evidence of it. To this end, I posed a challenge to controller manufacturers and they responded with a vengeance. My challenge was to provide their 2003 solution to the problem that plagued Fandrich in 1981 – perform a 30 g by 11 msec half-sine test on a shaker of 1 in. (PTP) stroke capacity while respecting all tolerance limits of MIL-STD-810C (yes, I know we’re up to F!).

Each manufacturer was asked to provide his solution as a versus-time Excel file. These have been collectively plotted in Figure 13. I think we learn from the similarities and from the differences. It is clear that the general form of alternating positive and negative compensation pulses before and after the test-pulse is common to all solutions. It is also clear that different designers have taken different routes to solving this problem, and solving it well.

Presenting Pulse Spectra Properly

Spectrum (FFT) analysis is applied to all kinds of signals. The appropriate amplitude scaling is different for periodic, random and transient signals. Measuring spectral amplitude in gs (or volts or any other transduced linear unit) is proper for a *periodic* signal or a mixed signal dominated by essentially stationary tones. The preferred scaling for this type of measurement is root-mean-square (rms) amplitude.

When a continuous *random* signal is measured, we require *power spectral density* (PSD) amplitude scaling in g^2/Hz to provide an instrument-independent amplitude description.

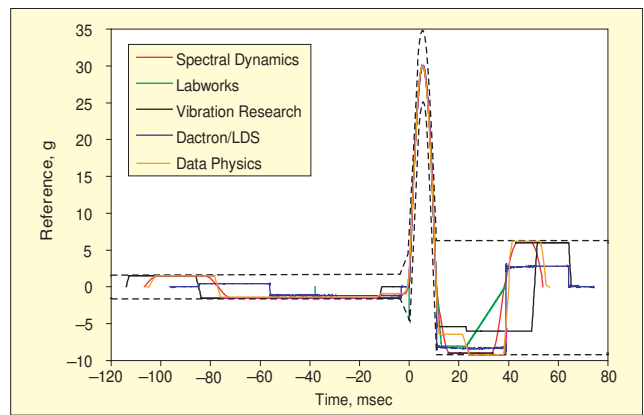


Figure 13. Current commercial solutions to the 30 g by 11 msec half-sine problem. Dashed lines – upper and lower bounds per MIL-STD-810C.

When a *transient* pulse is analyzed, the correct spectral amplitude unit is energy spectral density (EDS), expressed in g^2sec/Hz . Any other scaling provides an amplitude answer dependent on the specifics of the hardware making the measurement, never a desirable thing.

The area under a PSD curve is the continuous random signal’s *mean-square* value (overall-rms²), often termed the *signal power*. The area under an acceleration ESD curve is the *signal energy* defined by:

$$SE = \int_0^T \dot{y}^2 dt \quad (25)$$

The acceleration *signal energy* thus has units of g^2sec (or related acceleration and time units). This provides the ‘ g^2sec ’ portion of the g^2sec/Hz units of an ESD. The “per Hz” dimensional component is the same as that of a PSD, the *noise bandwidth* of the spectrum analyzer making the measurement. Table 1 lists the (total) *signal energy* of each pulse type discussed in this article as a normalized k_{SE} coefficient. Multiplying k_{SE} by the square of the pulse amplitude and the duration of the pulse (A^2T) provides the signal energy in physical units.

All spectral plots presented herein are normalized. The frequency axis is multiplied by pulse duration T , so that the horizontal axis is dimensionless. Energy spectral density is presented vertically. This is divided by AT^2 so that the vertical axis has dimension Hz^{-1} .

Figure 8 presents a comparison of the ESDs of the rectangular pulse and its band-limited Fandrich approximation. We will now examine the ESD spectra of the various *Classical Shock* excitation pulses.

In Figure 14, the half-sine pulse exhibits zeros at $1.5/T$, $2.5/T$, $3.5/T$ and so on. The first side-lobe is 23 dB below the maximum value and subsequent lobe peaks fall off at -12 dB/octave. The haversine (i.e. the Hanning window shape) has a broader primary lobe and more rapidly decaying side-lobes. Its first zero occurs at $2/T$ and subsequent zeros occur at integer multiples of $1/T$. The first side-lobe peak is -32.2 dB below the main lobe. Higher side-lobes decay at -18 dB/octave.

Figure 15 presents three traces, the triangle pulse, the initial-peak (IP) sawtooth and the terminal-peak (TP) sawtooth. As intuition might suggest, the spectral magnitudes of the IP and TP sawtooth waveforms are identical. (The corresponding *phase* spectra are reflections of one another as these two complex spectra are a conjugate pair.)

The triangle wave has wide lobes, with zeros occurring at integer multiples of $2/T$. The first side-lobe is -26.5 dB below the maximum and subsequent lobes attenuate at -12 dB/octave. In contrast, the sawtooth waveforms exhibit *no zeros*. The spectrum follows that of the triangle’s primary lobe to a frequency of $1/T$ and then rolls off smoothly at a rate of -6 dB/octave.

Figure 16 presents the damped-sine at three different damping levels ($\delta = 0.0, 0.2$ and 0.375 .) The undamped sine ($\delta = 0$) exhibits a unique primary lobe that starts with a zero at DC.

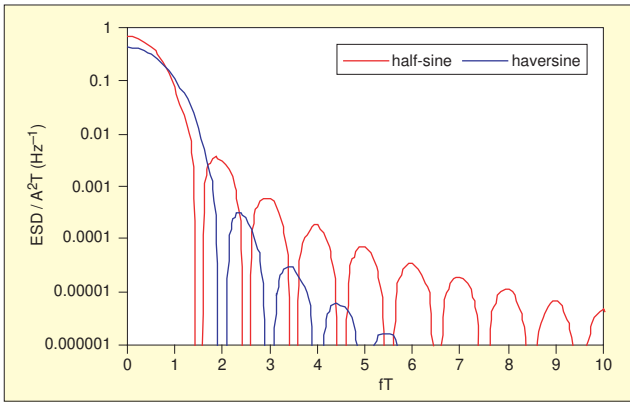


Figure 14. Comparison of the half-sine and haversine pulse spectra.

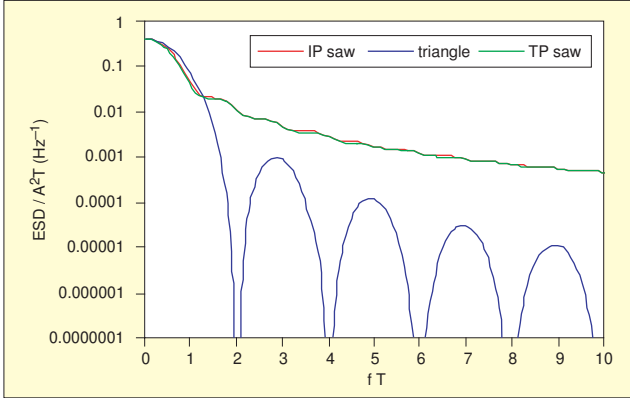


Figure 15. ESD spectra of sawtooth and triangle waveforms.

The upper-side of the primary lobe is bounded by a zero at frequency $2/T$. Subsequent zeros occur every $1/T$ thereafter. The first side-lobe is 18.3 dB lower than the primary, and following side-lobes diminish at the rate of -12 dB/octave.

As damping is added, the peaks and zeros become less definite and the spectrum eventually converges to a -12 dB/octave line (above frequency $= 1/T$) for high damping. As a matter of practicality, use of damping in excess of $\delta = 0.375$ is unlikely. At this value, k_D and k_V converge (see Figure 10) and their ratio remains unity while both diminish thereafter.

Many controllers provide for FFT spectrum analysis (as well as SRS analysis) of shock-test measurements. However, I am unaware of any current controller that properly scales the amplitude of such transient measurements to ESD format as a matter of course. This is an unfortunate omission as test labs continue to accumulate libraries of system-dependent g-versus-Hz documentation.

What causes damage?

The Holy Grail of package design is a means of predicting if a component or system will fail when exposed to a given shock pulse, *before applying the pulse*. I know of no one who claims to have this answer.

In a landmark work, Gaberson, et al² addressed the problem of what to measure during an observable shock to indicate the damage potential of the event. The proposed modification to the Shock Response Spectrum (SRS) algorithm has yet to be incorporated in any commercial controller or analyzer. Dr. Howard Gaberson has promised to apply these methods to investigate the effects of compensation pulses on damage potential, hopefully in a future issue of *Sound and Vibration*.

The previously mentioned *signal energy* (k_{SE}) coefficients of Table 1 and the corresponding *energy spectral density* distributions just discussed are probable inputs to the damage prediction process. However, signal energy is not synonymous with the *mechanical energy* input to a structure under test. The remaining non-dimensional coefficient k_{ME} in Table 1 attempts to estimate this.

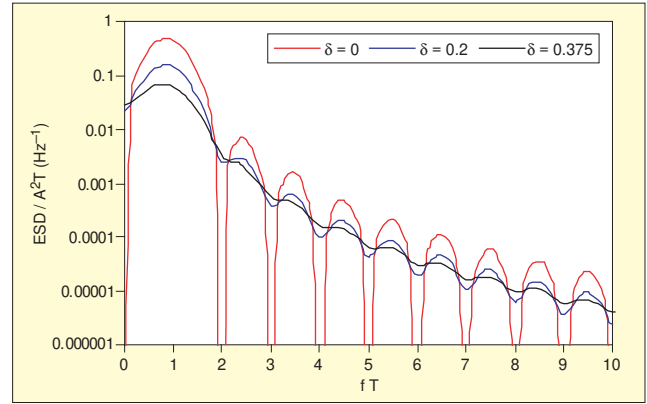


Figure 16. ESD spectra of damped-sine at various damping values δ .

The shaker applies a transient force equal to the test-mass acceleration product $F = M\ddot{y}$ to the device under test. The integral of this force with respect to the resulting displacement is the work done by the shaker on the test article, which must eventually equate to all resulting energy dissipated by the structure's *plastic* behavior. While some of the dissipation occurs without damage, the overall energy imparted to the test item seems a very likely index of damage potential.

k_{ME} is derived from:

$$MA^2T^2k_{ME} = ME = Work = \int_0^T F dx = \int_0^T F \frac{dx}{dt} dt = \int_0^T F \dot{y} dt = M \int_0^T \dot{y} \dot{y} dt \quad (26)$$

Looking at the k_{ME} values in Table 1 suggests that the Fandrich pulse is no less damaging than the rectangle it replaces. It further implies that either of these pulses is four times as likely to produce a failure as a haversine, triangle or sawtooth of the same peak value and duration. It also denotes a half-sine as being 162% as aggressive as a haversine of like proportion. Does this simple one-number statistic provide a harbinger of potential failure? I suspect not, reflecting on the observation that a full-sine pulse has a k_{ME} equal to zero.

However, k_{ME} in consort with other pulse (and structural) properties may provide a few more lumens as we chart the dark cave of transient-induced mechanical failure.

Closure

This article has reviewed shock-testing on shakers from several aspects. It has provided some lessons in basic physics, in signal processing and in the history of our industry. It has also given many manufacturers dedicated to our industry an opportunity to demonstrate their committed support of our work through their own research and development. I thank them for their candor and trust in contributing to this article.

References

1. R. Fandrich, "Optimizing Pre- and Post-Pulses for Shaker Shock Testing," *The Shock and Vibration Bulletin*, Number 51, Part 2, May 1981.
2. H. Gaberson, D. Pal, and R. Chapler, "Classification of Violent Environments That Cause Equipment Failure," *Sound and Vibration*, Volume 32, Number 5, May 2000.
3. W. E. Frain, "Shock Waveform Testing on an Electrodynamics Vibrator," *The Shock and Vibration Bulletin*, September 1977.
4. R. Lax, "A New Method for Designing MIL-STD Shock Tests," *Test Engineering & Management*, June/July 2001. 

The author can be contacted at george@foxlang.com.